In situ spectroscopic investigation of low-temperature oxidation of methane over alumina supported platinum during periodic operation

Elin Becker[a], Per-Anders Carlsson[a],* Lisa Kylhammar[a], Mark A. Newton[b], and Magnus Skoglundh[a]

[a]*Department of Chemical and Biological Engineering and Competence Centre for Catalysis, Chalmers University of Technology, SE-412 96 Göteborg, Sweden*

[b]*European Synchrotron Radiation Facility, Grenoble, France*

E-mail: per-anders.carlsson@chalmers.se

Abstract

Methane oxidation over Pt/Al_2O_3 at transient inlet-gas conditions was studied *in situ* using synchronous EDXAS, FTIRS and mass spectrometry. The employed combination of experimental techniques allows for simultaneous analysis of, respectively, the electronic state of platinum, surface coverage of reaction intermediates/products and catalytic activity/selectivity. By cycling of the feed gas composition between net-oxidizing and net-reducing conditions the activity for methane oxidation can be increased as compared to continuous net-oxidising conditions. Using the white-line area of time-resolved XANES spectra, a quantitative estimation of the surface O/Pt ratio indicates the formation of an inhomogeneous surface oxide on the platinum crystallites during reaction. The obtained temporary high activity can be explained

*To whom correspondence should be addressed

through Langmuir-Hinshelwood kinetics and may result either from the formation of a partially oxidized platinum surface that is more effective for methane dissociation or, more likely, from a period with more reactive chemisorbed oxygen prior to oxide formation.

Introduction

The use of methane in energy conversion processes is expected to increase[1] because it is available in abundant quantities as natural gas[1,2] and, more preferably, CH_4 can be produced from biological feedstocks yielding biogas.[3] Combustion of methane forms less carbon dioxide per produced quantity of energy compared to other hydrocarbons[4,5] and the resulting emissions often contain relatively low levels of nitrogen oxides and particulates.[6] Thus, combustion of methane may offer an attractive alternative to conventional combustion of, e.g., petrol and diesel, for both industrial and automotive applications. However, as methane is a strong greenhouse gas[7] the complete design of methane combustion processes must target low methane emissions. In this connection we consider here one important strategy, namely, conversion of methane emissions through catalytic total oxidation.

Methane is the most stable hydrocarbon and consequently catalytic oxidation of methane requires relatively high temperatures to proceed with an acceptable rate. This is so even for the most active catalysts like supported Pd and/or Pt.[8,9] In terms of elementary steps, the low activity is related to the difficulty associated with the dissociative adsorption of methane on catalyst surfaces.[10] The sticking probability of methane on noble metals is low,[11] and in addition, methane dissociation is strongly dependent on the surface coverage of reaction intermediates. Studies on CH_4 oxidation over Pt/Al_2O_3 under transient reaction conditions indicate that unfavorably high oxygen coverage inhibits the CH_4 dissociation leading to significantly low activity for total oxidation.[12,13] As a means to overcome such inhibition effects, periodic operation, i.e., alternating between net-oxidizing and net-reducing characteristics of the feed gas, can be employed.[12] Notably in such experiments, the conversion of methane is surprisingly high just after the switches.

The reason for this is presently unclear. Considering for example the oxidation of CH_4 to obey Langmuir-Hinshelwood (LH) kinetics,[13,14] the transient high activity may result from a transition through a state with favorable adsorbate composition during the gas switch.[13] Another explanation may involve changes of the electronic state of the catalyst surface, as a response to the changing gas atmosphere, which crucially can influence the catalytic activity. To test these hypotheses, we carried out experiments of CH_4 oxidation over Pt/Al_2O_3 under transient reaction conditions using *in situ* energy dispersive x-ray absorption spectroscopy (EDXAS) in combination with mass spectrometry (MS). EDXAS is a powerful technique for analysis of electronic structures of condensed matter, e.g., the chemical state of platinum, and is thus used in many fields of research including chemical sensors, semiconductors and catalysts. By developing a method for analysis of the so-called white-line in Pt L_{III} edge spectra, in the x-ray absorption near-edge structure (XANES) region, we were able to qualitatively correlate even small changes in surface O/Pt ratio with significant changes in catalytic activity.[15] The term surface O/Pt ratio was introduced to account for oxygen in any type of platinum-oxygen species as IUPAC definitions provide no clear distinction between adsorbed oxygen and platinum oxides.[16]

In the present study we revisit oxidation of methane over Pt/Al_2O_3 at transient reaction conditions. Our focus is on the mechanistic consequences of periodic operation and the dynamic behavior of platinum to obtain increased understanding of the origin of the transient high activity. By using synchronous, time-resolved, EDXAS and Fourier transform infrared spectroscopy (FTIR) in combination with MS, we achieve complementary *in situ* information to connect changes in the electronic state and surface coverage of platinum with changes in catalytic activity. Specifically, we approach a quantitative analysis of the white-line region facilitating the mechanistic understanding of methane oxidation over alumina supported platinum.

Experimental section

Catalyst preparation and characterization

A 4%Pt/Al_2O_3 catalyst was prepared by wet impregnation. The support material, 3.8 g γ-Al_2O_3 (SCC a-150/200, Sasol), was dispersed in 10 g distilled water and the pH was adjusted to 2.5 by adding diluted HNO_3 solution (Merck). An aqueous platinum nitrate solution ($Pt(NO_3)_2$, 0.15 wt-%, Johnson Matthey) was added dropwise to the alumina slurry under continuous stirring to yield the desired Pt loading. The slurry was kept under continuous stirring for 20 min, frozen with liquid nitrogen and freeze dried. In order to preserve a high Pt dispersion, the catalyst was calcined at 450 °C for 4h in air, starting with a temperature ramp from room temperature with a rate of 5 °C per minute to 450 °C. The platinum dispersion of the final catalyst was determined by CO chemisorption (Micromeritics, ASAP2010C) at 27 °C giving 65% dispersion assuming a maximum CO/Pt ratio of 0.8, which is reasonable for highly dispersed Pt particles.[17] The BET surface area (Micromeritics, Tristar) of the sample was measured to be 182 m^2/g.

Synchronous *in situ* EDXAS/FTIR/MS measurements

Synchronous, time resolved, EDXAS/FTIR/MS measurements were performed *in situ* at beamline ID24 at the European Synchrotron Radiation Facility (ESRF) in Grenoble, France. The experimental set-up was designed for precise transient studies through the combination of air actuated high-speed gas valves (Valco, VICI) and a small reactor volume facilitating rapid gas composition changes over the catalyst sample. A Spectratech reaction cell modified for simultaneous EDXAS and FTIR spectroscopy in diffuse reflectance (DRIFTS) mode, see[18] for details, was used. About 40 mg of the Pt/Al_2O_3 sample was loaded into the sample cup which was 4 mm in diameter and 2.5 mm deep. For EDXAS, an Si[3 1 1] polychromator in Bragg configuration and a FReLoN detector[19] were used to follow the Pt L_{III}-edge at 11.564 keV. The expected $\Delta E/E$ is about 1 x 10^{-4} and thus an energy resolution of 1.2 eV is reasonable. The x-ray spot size on the sample was about 7 μm (FWHM) in the horizontal direction, whereas in the vertical direction the beam was

defocused from a standard 100 μm (at the detector) to about 300 μm in accordance with practice established for the study of spatially non-uniform samples at ID24.[20] The EDXAS data sampling time was 100 ms. A platinum foil (Goodfellow, 99.99% purity) was used for energy calibration of the obtained spectra and reference measurements were also peformed using PtO_2 (Johson Matthey, 99.95% purity). The EDXAS measurements were made at the top (gas inlet) of the sample bed to coincide with the volume sampled by the infrared measurements as best as is possible. The DRIFT spectra were recorded using a Bruker IFS infrared spectrometer equipped with a high sensitivity narrow band MCT detector. The product stream was analyzed by mass spectrometry (Pfeiffer, Prisma) following the m/z signals 2 (H_2), 4 (He), 15 (CH_4), 28 (CO), 32 (O_2) and 44 (CO_2).

Step- and pulse-response experiments

Oxygen step- and pulse-response experiments were carried out at 400, 360, 320 and 280°C as follows. The sample was treated with 1.5% O_2 at 400°C, cooled to the temperature to be studied and exposed to 0.1%CH_4 for 15 min. The step-response experiment was then started by switching the gas composition to 1.5%O_2/0.1%CH_4, hereafter referred to as a rich-lean (RL) switch, followed by a switch back to 0.1%CH_4, a lean-rich (LR) switch. The catalyst was exposed to each gas composition for a duration of 7 minutes. Subsequently, the pulse response experiment was triggered. Here the feed gas composition was repeatedly switched between 0.1% CH_4 for 1 min and 1.5%O_2/0.1%CH_4 for 1 min for a total duration of 20 min. In all experiments He was used as carrier gas and the total gas flow was kept constant at 100 ml/min throughout the study.

Results

Typical data obtained from the used spectroscopies is shown in Figure 1, here as three-dimensional representations of the evolution of XANES Pt L_{III}-edge spectra (left) and IR bands in the interval 1500-4000 cm^{-1} (right) during a pulse-response experiment. In the following we condense such data into two-dimensional representations for clearer visualization. Figure 2 shows x-ray absorp-

tion spectra for the Pt L_{III} edge recorded after a LR switch at 360 and 280°C. The spectra are extracted from the pulse-response experiments shown in Figure 4 and Figure 5 which will be discussed in more detail below. The shape of the spectra is characteristic for the XANES region at the Pt L_{III} edge. The intensity of the white-line decreases when the oxygen supply is switched off indicating a decreasing O/Pt ratio in line with previous studies.[15,21–23] The difference in white-line intensity in the presence and absence of oxygen, i.e., the topmost and lowest spectra for the respective temperature in Figure 2, is larger at 360°C as compared to 280°C. In the further analysis of XANES data, we use the white-line area (WLA)[15] as a measure of changes of the white-line intensity. Although the changes in white-line intensity in the present experiments are rather clear, we use this approach as analysis of also small changes in the spectra is facilitated, i.e., the transient responses can be analyzed more precisely. Additionally, the WLA method is less sensitive towards normalization of spectra as compared to other methods based on e.g. the white-line height or position of the inflection point of the white-line step.

Figure 3 shows the DRIFT spectra recorded when the sample is exposed to 0.1%CH_4 at 400, 360, 320 and 280°C. The IR absorption band positioned around 2046-2069 cm^{-1} is assigned to CO linearly bonded to Pt.[24–27] In the following we denote this band with $\tilde{\nu}_{lin}^{CO}$(Pt). The increase in intensity of the $\tilde{\nu}_{lin}^{CO}$(Pt) band with decreasing temperature reflects an increasing CO coverage on platinum. The observed shift of the IR band from 2046 to 2069 cm^{-1} with increasing IR absorption is partly an effect of less back donation of electrons to CO and partly due to increasing repulsive CO-CO lateral interactions with increasing CO coverage, see ref.[28] and references therein. At 280°C, also a band corresponding to CO bridge-bonded to Pt can be observed at about 1850 cm^{-1}. The IR absorption bands around 1500 cm^{-1}, here observed only at 400°C, are likely due to the presence of various types of carbonate species on the alumina support.[29]

In Figure 4 the results from the pulse-response experiment at 360°C are shown. The two upper panels display the MS data for the outlet stream together with the carbon balance while the two bottom panels show, respectively, the WLA for the Pt L_{III} edge and the intensity of the $\tilde{\nu}_{lin}^{CO}$(Pt) band. The latter is obtained through integration of the IR spectra between 1950-2080 cm^{-1}. In

general, changes of the oxygen concentration alter the reaction kinetics so that during oxygen excess, for example between t=5.8 and 6.8 min, total oxidation of methane into CO_2 and H_2O is favored while at periods with oxygen deficiency, e.g., t=6.8 to 7.8 min, partial oxidation of methane into mainly CO and H_2 is the main route. The transitions between total and partial oxidation are of course connected to changes in gas stoichiometry. More interesting, however, is the temporary high activity for total oxidation of methane caused by the gas changes. The minimum in CH_4 concentration at t=6.0 min, i.e. 0.2 min after oxygen is introduced and the maximum in CO_2 concentration at t=7.0 min, i.e., 0.2 min after O_2 is switched off, give evidence for the high activity. Considering the results in more detail, the temporary high activity is connected to changing surface conditions. At the introduction of an oxygen pulse, for example at t=5.8 min in Figure 4, the concentration of CO_2 starts to increase rapidly for about 0.2 min, passes through a maximum and declines towards 0.04 % for the remaining time of the oxygen pulse. The simultaneous increase in methane concentration in the beginning of this phase is commented on further below. During the first 10 s, the increase in CO_2 concentration is primarily due to oxidation of accumulated CO on platinum as indicated by the rapid decrease in CO coverage, i.e., the intensity of the $\tilde{\nu}_{lin}^{CO}$(Pt) band drops abruptly to a negligible level. Some thermal desorption of CO caused by reaction exothermicity may occur even though this contribution likely is minor. At the same time, the O/Pt ratio increases, rapidly at first, as evidenced by the sharp increase in WLA and then the increase in WLA flattens out for the remaining time with oxygen exposure. During the period where the WLA increases rapidly, the CO_2 concentration increases further through a maximum reflecting oxidation of carbon containing species accumulated on the platinum surface. The similar profile of the carbon balance supports a net-release of carbon into the gas phase. Thus, during this period the surface coverage changes considerably from a state where carbon containing species on the surface are most abundant to a state where oxygen dominates the surface. However, the change in surface conditions triggers a temporary high activity for methane oxidation evidenced by the methane concentration passing a minimum at t=6.0 min. From the carbon balance and WLA it is clear that this transient high activity appears after the majority of the accumulated carbon species

have been oxidized but before the highest O/Pt ratio is reached. Further oxygen exposure leads to oxygen poisoning thus the methane concentration levels out, here at about 0.065%. The minimum in CH_4 concentration observed here is not as pronounced in terms of absolute levels and duration as previously observed.[12] The reason for this is mainly due to the higher feed of oxygen in relation to both the concentration of CH_4 and amount of catalyst in the present study, leading to a more rapid change of the surface conditions, i.e., oxygen poisoning. The transient high activity can be elaborated on by varying the gas flow and composition as well as pulse duration/frequency. However, in this study, the main focus is on connecting catalytic activity to surface composition and to conceptually understand the mechanistic consequences of periodic operation rather than on optimizing the conversion of methane. At t=6.8 min in Figure 4 where the oxygen supply is switched off, the methane concentration and WLA start to decrease simultaneously. The decrease in CH_4 concentration is quite rapid partly due to accumulation of carbon containing species on the catalyst as indicated by the carbon balance. However, the decrease in WLA is at first rather slow and then more rapid at around t=7.0 min. Interestingly, a maximum in CO_2 concentration indicates again a transient high activity due to changing surface conditions, at this time, from an oxygen rich state to a state where carbon containing species are most abundant. This is also observed by the increasing coverage of CO through the evolution of the $\tilde{\nu}_{lin}^{CO}$(Pt) band. Besides accumulation of carbon containing species, the increasing concentrations of CO and H_2 in this phase reflect the change from total to partial oxidation of CH_4 as the main route for conversion of methane.

The transient behavior for the pulse-response experiments at 400, 320 and 280°C are qualitatively similar to the case of 360°C. The absolute concentration levels of reactants and products and the intensity of WLA and the $\tilde{\nu}_{lin}^{CO}$(Pt) band are of course different as the rates for the involved processes change with temperature. For example, lower temperature means lower methane conversion between switches which also makes the transient high activity visually more clear, *cf.* Figure 5. Furthermore, the effect of poisoning either by carbon containing species or oxygen is more pronounced at low temperatures. One difference, though, is the evolution of the $\tilde{\nu}_{lin}^{CO}$(Pt) band. In contrast to the case of the higher temperature described above, this band increases and flattens out

at a steady level at the lower temperatures (320 and 280°C) in this study.

To observe more clearly the full responses to gas composition switches, both RL and LR step-response experiments at 400, 360, 320 and 280 °C were performed. Here, we show in Figure 6 and Figure 7 the results for 360 and 280°C in the case of RL and LR switches. Analogous to the pulse-response experiments, the upper panels display the MS data for the outlet stream together with the carbon balance while the two bottom panels show the WLA for the Pt L_{III} edge and the intensity of the $\tilde{\nu}_{lin}^{CO}$(Pt) band. The general trends with transient high activity after the switches are the same as for the corresponding pulse-response experiments and are not commented on further here. As the step-response experiments reach almost stationary conditions the absolute levels of the measured quantities are somewhat different in comparison to the pulse-response experiments. For example in Figure 6 a higher CH_4 concentration is reached. Also, the WLA reaches higher values as does the transient production of CO_2. For the LR switch in Figure 7, the main difference compared to the pulse-response experiments is that the CO concentration approaches zero.

Discussion

Synchronous, time-resolved, *in situ* XANES/DRIFTS/MS have been used to study the kinetics of oxidation of methane over Pt/Al_2O_3 at transient conditions. The employed combination of experimental techniques facilitates simultaneous analysis of, the electronic state of platinum, surface coverage of reaction intermediates and catalytic activity/selectivity. The study was carried out in the pure kinetic regime, i.e., without diffusion limitations, thanks to the use of a specially designed reactor cell and careful choice of the physical properties of the catalyst and reactions conditions (*cf.* Appendix). Thus, we discuss the results in terms of kinetic events focusing on the mechanistic consequences of periodic operation and the dynamic behavior of platinum, i.e., transitions between metallic and oxide phases, during transient methane oxidation. The latter involves an approach towards quantitative interpretation of the Pt L_{III} XANES region. Finally, the possibility of an effective oxygen storage in the Pt/Al_2O_3 system is briefly commented on.

The MS data demonstrate that efficient oxidation of methane with oxygen over Pt/Al_2O_3 is a delicate balancing act of achieving a suitable composition of the reactants in the feed gas. For example, the catalytic activity for stationary lean conditions at temperatures below 400°C is generally quite low whereas introduction of rich periods through rich-lean cycling results in temporary high activity and thus, on average, an increased conversion of methane. These observations indicate, in line with previous studies,[8,30] a sensitivity towards oxygen poisoning which effectively can be reduced through cycling of the feed gas composition.[12,13,15,31] In terms of surface kinetics, the rate-determining step for methane oxidation is generally considered to be the dissociative adsorption of methane.[10] This activated process depends not only on the catalyst surface, for example the initial sticking probability is higher on the low-coordinated Pt[533] plane as compared to the close-packed Pt[111] surface,[32] but also on the actual coverage of reaction intermediates on the surface.[33,34]

Assuming the oxidation of methane on platinum to follow Langmuir-Hinshelwood type of kinetics, i.e., reactions between adsorbed species only, the observed temporary high activity may be the result of a period with favorable competition between dissociative adsorption of CH_4 and O_2 through their respective surface coverage dependent sticking probabilities. In the case of an RL-switch, the oxygen coverage builds up, eventually reaching a critical point where the dissociative adsorption of methane is significantly reduced, thus leading to low activity for methane oxidation. Several studies on Pt single crystals indicate that even low coverages of oxygen hinder the dissociative adsorption of methane.[33,35,36] This interpretation suggests that the observed changes in WLA primarily reflect changes in oxygen coverage. As the activity maxima in Figure 4 and Figure 5 occur for intermediate values of the WLA, this reasoning implies that dissociation together with further oxidation of methane is favored on surfaces with intermediate coverages. In this connection, Burch *et al.*[10] speculated on the possibility of a more efficient activation of the C-H bond for dissociation via heterolytic splitting through the polarization of the CH_4 molecule by the partially oxygen covered platinum surface.[10] Further, Kondo *et al.* report that the oxidation probability is higher on the Pt[111]-(2×2)-O surface as compared to CH_4 dissociation on the Pt[111] surface.[37]

Taking the observations by Burch *et al.* and Kondo *et al.* into account, the Langmuir-Hinshelwood type of kinetics thus need to be complemented, also considering the active state of platinum in order to explain the observations in the present study.

It is generally accepted that the white-line of Pt L_{III} spectra can be used for analysis of the degree of oxidation of supported Pt particles, and the interpretation is that a higher absorption reflects a more oxidized sample. For example Yoshida *et al.* used this approach to study the effect of different support materials on the oxidation state of Pt[38] and Grünwaldt *et al.* to study the ignition and extinction process of catalytic partial oxidation of methane.[39] Various methods for qualitative analysis of the white-line have previously been proposed and we have in this connection developed a sensitive method based on analysis of the white-line area. Although not straightforward, we here attempt to advance our analysis of the WLA towards quantitative interpretation by using reference measurements of Pt foil and PtO_2. The Pt foil is considered to represent the pure metallic state of platinum although a thin oxide layer may have formed on the surface. However, the contribution of such an oxide layer on the WLA is expected to be negligible. In the case of PtO_2, the platinum is considered to be completely oxidized thus representing the Pt^{4+} state. The WLA for the Pt foil and PtO_2 was measured to be, respectively, 1.3 and 10.4. With the assumption of a linear relationship between the WLA and the oxidation state of platinum, in analogy with the study by Yoshida *et al.*,[21] the Pt^{2+} state, i.e. PtO, would correspond to a WLA of 5.2. Furthermore, for our sample having 65% platinum dispersion, a surface O/Pt ratio of one would correspond to a WLA of 3.4. Considering again the CH_4 oxidation experiments, the maximum WLA at 280 and 360°C is 1.8 and 3.2 corresponding to, respectively, a surface O/Pt ratio of about 0.5 and slightly below 1.0. The estimated sensitivity is 0.1 monolayers of oxygen on Pt. Assuming a homogeneous distribution of oxygen on the platinum surface, this may be interpreted as submonolayers of chemisorbed oxygen. However, at the temperatures studied here, the oxygen desorption is considerable implying that the coverage of oxygen is determined by the oxygen adsorption-desorption equilibrium. This favors a decrease in the oxygen coverage, i.e., a decrease in WLA, with increasing temperature in contrast to our observations. Also the distribution of oxygen on the surface is likely neither homo-

geneous nor restricted to chemisorbed species, thus the local O/Pt ratio may be higher reflecting the presence of surface oxide islands. A closer examination of the IR spectra collected at 280 and 360°C reveals a shift towards higher wavenumbers of the $\tilde{\nu}_{lin}^{CO}$(Pt) absorption band upon an LR-switch. Also, comparing the two temperatures, the evolution of the $\tilde{\nu}_{lin}^{CO}$(Pt) absorption band is different. The shift is, in analogy with Figure 3, due to an increasing surface coverage of CO. On the other hand, a shift towards lower wavenumbers signifying the reduction of platinum oxide by CO was previously observed for CO oxidation on Pt/Al_2O_3.[28] The reason why a similar shift is not observed here, despite the simultaneous decline in WLA is likely due to the much lower concentration of CO in the present experiments. The formed CO is preferentially adsorbed on metallic platinum sites indicating an inhomogeneous distribution of surface oxides.[40] The partial reduction of the platinum surface during the initial 10 s after oxygen is switched off thus results in CO_2 formation and hence total oxidation of CH_4. At 400 °C (not shown), it is clear that oxidation of the Pt crystallites occurs. For this temperature the WLA reaches 4.0 corresponding to a surface O/Pt ratio considerably higher than one. The oxide formation seems more likely as the observed WLA is higher at the higher temperatures which is anticipated from an activated oxidation process. The transient high activity may then, according to the scenario with oxide formation, either result from a partially oxidized Pt surface that can dissociate methane more effectively than a metallic surface, analogous to the case of heterolytic C-H splitting discussed previously. However, this is not in line with the continuously increasing O/Pt ratio together with the decreasing methane dissociation during the rich periods in our experiments. It is more likely that the transient high activity is caused by a period with more reactive chemisorbed oxygen before the formation of a surface platinum oxide with lower activity for methane oxidation. One should mention that although the dissociative adsorption of methane is the rate-determining step, the most active surfaces for methane oxidation is not necessarily the same as the most active surfaces for methane dissociation as the former refers to the entire catalytic cycle whereas methane dissociation is only one step in that cycle. The different evolution of the $\tilde{\nu}_{lin}^{CO}$(Pt) absorption band at the two temperatures is probably a result of different relative rates of the involved reaction steps at 280 and 360°C. Specifically, the relation

between the rate of methane dissociation and further reaction to CO and the rate of CO desorption may be different. In fact during the oxygen-free periods, the CO coverage reflects the balance of formation and desorption of CO. In the case of 360°C, the oxygen switch off leads to an initial accumulation of adsorbed CO due to that the methane dissociation and further reaction to CO is more rapid than the CO desorption. After a certain period the CO formation decreases as oxygen is consumed. During this stage also other carbon containing species that are weekly or non-IR active, e.g., carbon, form on the surface. The CO desorption, however, remains high during this period eventually leading to a decreasing CO coverage. In contrast, at the lower temperature, the CO coverage is relatively high and remains high during the oxygen-free periods indicating that the CO desorption is significantly lower at this temperature.

In both the step- and pulse response experiments, significant CO production is observed during the rich periods, i.e., when no oxygen is supplied via the feed gas. This is particularly evident in the step-response experiments where the oxygen supply is switched off during 10 min and for which CO starts to form after the first minute and is observed throughout the experiment. The oxygen required to produce CO must in this case originate from the catalyst. Since we observe a reduction of the platinum upon switching off the oxygen it is likely that at least a part of the oxygen is supplied from the platinum crystallites in the catalyst. However, quantitative analysis of the WLA indicates that this cannot be the only source of oxygen. For example, at 360°C the maximum WLA is 3.2 which according to previous analysis corresponds to nearly a monolayer of oxygen. In the 40 mg sample bed the amount of surface Pt is estimated to be 5.3 μmoles. The produced amount of CO corresponds to 8.5 μmoles, thus, about 3.2 μmoles oxygen equivalents origin from other oxygen containing species in the Pt/Al_2O_3 system. The corresponding calculations for other temperatures qualitatively show the same results. This is in line with a previous study,[13] where the inclusion of an effective oxygen reservoir was necessary to accurately reproduce the experimental results. The fact that the WLA remains fairly constant during the rich phase of the experiments renders it unlikely that the oxygen originates from the platinum crystallites. Instead, it seems more likely that oxygen is supplied from the alumina support where it may have been stored as

hydroxyl-groups or carbonates. In the IR spectra, we do observe absorption bands associated with carbonates on the alumina support at 400°C, however not at the other temperatures studied. The regions where one usually observes the absorption bands for hydroxyl-groups and carbonates are unfortunately rather noisy, which may obscure the existence of such species.

In summary, the present study confirms that the sensitivity towards oxygen poisoning of methane oxidation over platinum effectively can be reduced through cycling of the feed-gas composition, which favors the dissociative adsorption of methane. The temporary high activity can be explained by a period of favorable competition between dissociative adsorption of methane and oxygen following LH kinetics. Further, the increase in activity may also result either from the formation of a partially oxidized platinum surface that can dissociate methane more effectively as compared to a more metallic Pt surface, or more likely, from a period with more reactive chemisorbed oxygen, prior to oxide formation.

Concluding remarks

We have used a combination of *in situ* EDXAS, FTIRS and mass spectrometry to study methane oxidation over Pt/Al_2O_3 at transient inlet-gas conditions. The employed combination of experimental techniques facilitates simultaneous analysis of, respectively, the electronic state of platinum, surface coverage of reaction intermediates and catalytic activity/selectivity. Our results show that the activity for methane oxidation can be increased through cycling of the feed gas composition between net-oxidizing and net-reducing conditions, which favors dissociative adsorption of methane. Both the surface composition and the active state of the catalyst are affected by the transients, resulting in increased activity for methane oxidation when switching on and off oxygen in the feed. Using the white-line area of the time-resolved XANES spectra, a quantitative estimation of the surface O/Pt ratio indicates the formation of an inhomogeneous surface oxide on the platinum crystallites during reaction. The obtained temporary high activity can be explained through Langmuir-Hinshelwood kinetics and may result either from the formation of a partially oxidized

platinum surface that is more effective for methane dissociation or, more likely, from a period with more reactive chemisorbed oxygen prior to oxide formation. The results further indicate that periodic operation is a potential strategy to increase the methane conversion during oxygen excess in emission control.

Acknowledgement

This work has been performed within Swedish Research Council Proj. no. 621-2005-3592 and the Competence Centre for Catalysis, which is hosted by Chalmers University of Technology and financially supported by the Swedish Energy Agency and the member companies AB Volvo, Volvo Car Corporation, Scania CV AB, Saab Automobile Powertrain AB, Haldor Topsøe A/S, and The Swedish Space Corporation. The authors thank the European Synchrotron Radiation Facility (ESRF), Grenoble, France, for providing the beamtime.

Appendix

The influence of external (gas phase) diffusion limitations on the reaction rate can be estimated by calculating the difference in CH_4 concentration between the gas bulk and the surface of the catalyst grains (ΔC_{CH_4}). First we note that the observed reaction rate approximately is,

$$r_{obs} = q\frac{p_{CH_4}}{RT}\frac{X}{W}, \tag{1}$$

where q is the volumetric flow rate at room temperature ($1.67 \cdot 10^{-6}$ m^3/s), p_{CH_4} is the partial pressure of CH_4 (10^2 Pa), R is the molar gas constant (8.31 J/(mol K), T is temperature (300 K), X is the CH_4 conversion (0.6) and W is the amount of catalyst ($4 \cdot 10^{-5}$ kg). Substituting the given values one obtain $r_{obs} = 1.0 \cdot 10^{-3}$ mol/(s kg catalyst). For a packed-bed reactor with spherical catalyst grains at steady-state conditions, the reaction rate is coupled to the film-transport by,

$$r = S_m k_c \Delta C_{CH_4}, \tag{2}$$

where $S_m = 6/d_g\rho_g$ is the external surface area of the grain per mass of grain and d_g and ρ_g are the grains diameter and density, respectively. $k_c = ShD_{AB}/d_p$ is then the mass transfer coefficient where Sh is the Sherwood number and D_{AB} the binary gas diffusivity. Solving for ΔC_A gives,

$$\Delta C_{CH_4} = \frac{r d_g^2 \rho_g}{6ShD_{AB}}. \tag{3}$$

Substituting r_{obs} for r and assuming a reasonable low value for the Sherwood number ($Sh = 1.5$) will produce an estimate of the largest concentration gradient. Using $d_g = 125 \cdot 10^{-6}$ m^2, $\rho_g = 1.5 \cdot 10^3$ kg/m^3, $D_{AB} = 8.1 \cdot 10^{-5}$ m^2/s one arrives at $\Delta C_{CH_4} = 3.2 \cdot 10^{-5}$ mol/m^3 which is negligible compared to the concentration in the gas bulk, $C^b_{CH_4} = p_{CH_4}/(RT) = 1.8 \cdot 10^{-2}$ mol/m^3

at T=673 K.

The influence of internal diffusion limitations in a porous catalyst can be estimated by calculating the Weisz modulus,

$$\Phi = \frac{r_v r_g^2}{C^s_{CH_4} D_{eff}}, \tag{4}$$

where r_v is the reaction rate per volume of catalyst, r_g is the grain radius, $C^s_{CH_4}$ is the CH_4 concentration at the surface of the grain and D_{eff} is the effective diffusivity. The Weisz-Prater criterion can then be used, i.e for an isothermal spherical catalyst grain and a first-order reaction, $\Phi < 1$ implies a particle free from internal concentration gradients. This corresponds to a high efficiency factor, $\eta \geq 0.95$.

Since the external diffusion limitations are negligible the concentration at the surface of a catalyst grain is well approximated with the concentration in the gas bulk, hence,

$$\Phi = \frac{r_{obs} \rho_{cat} r_g^2}{C^b_{CH_4} D_{eff}}, \tag{5}$$

where $r_{obs} = 1.0 \cdot 10^{-3}$ mol/(s kg catalyst), $\rho_g = 1.5 \cdot 10^3$ kg/m^3, $r_g = 62.5 \cdot 10^{-6}$ m^2, $C^b_{CH_4} = 1.8 \cdot 10^{-2}$ mol/m^3 and $D_{eff} = 3.8 \cdot 10^{-7}$ m^2/s gives $\Phi \approx 0.87 < 1$ indicating the absence of internal diffusion limitations.

References

(1) Siddiqi, T. A. *Energy Policy* **2002**, *30*, 1145.

(2) Afgan, N. H.; Pilavachi, P. A.; Carvalho, M. G. *Energy Policy* **2007**, *35*, 704.

(3) Huber, G. W.; Iborra, S.; Corma, A. *Chem. Rev.* **2006**, *1006*, 4044.

(4) Han, J.; Zemlyanov, D.; Ribeiro, F. *Catal. Today* **2006**, *117*, 506.

(5) Ciuparu, D.; Lyubovsky, M.; Altman, E.; Pfefferle, L.; Datye, A. *Catal. Rev.* **2002**, *44*, 593.

(6) P. Gélin, M. P., L. Urfels; Tena, E. *Catal. Today* **2003**, *83*, 45.

(7) IPCC, Climate change 2001:, The Scientific Basis. Ch 6.12 Global warming potential, Cambridge University Press, London (2001), p. 385.

(8) Burch, R.; Loader, P. *Appl. Catal. B* **1994**, *5*, 149.

(9) Garetto, T. F.; Apesteguia, C. R. *Catal. Today* **2000**, *27*, 243.

(10) Burch, R.; Hayes, M. *J. Mol. Catal. A: Chem.* **1995**, *100*, 13.

(11) Burch, R.; Crittle, D.; Hayes, M. *Catal. Today* **1999**, *47*, 229.

(12) Carlsson, P.-A.; Fridell, E.; Skoglundh, M. *Catal. Lett.* **2007**, *115*, 1.

(13) Carlsson, P.-A.; Nordström, M.; Skoglundh, M. *Top. Catal.* **2009**, *52*, 1962.

(14) Hickman, D. A.; Schmidt, L. D. *Science* **1993**, *259*, 343.

(15) Becker, E.; Carlsson, P.-A.; Grönbeck, H.; Skoglundh, M. *J. Catal.* **2007**, *252*, 11.

(16) Burwell, R. *Adv. Catal.* **1977**, *26*, 351.

(17) Lööf, P.; Kasemo, B.; Andersson, S.; Frestad, A. *J. Catal.* **1991**, *130*, 181.

(18) Newton, M. A. *Top Catal* **2009**, *52*, 1410.

(19) Labiche, J. C.; Mathon, O.; Pascarelli, S.; Newton, M. A.; Ferre, G. G.; Curfs, C.; Vaughan, G.; Homs, A.; Carreiras, D. F. *Rev. Sci. Instrum.* **2007**, *78*, 091301.

(20) Newton, M. A. *J. Synchrotron Rad.* **2007**, *14*, 372.

(21) Yoshida, H.; Nonoyama, S.; Yasawa, Y.; Hattori, T. *Physica Scripta* **2005**, *T1115*, 813.

(22) Beck, I.; Bukhtiyarov, V.; Pakharukov, I. Y.; Zaikovsky, V. I.; Kriventsov, V. V.; Parmon, V. *J. Catal.* **2009**, *268*, 60.

(23) Meitzner, G.; Via, G. H.; Lytle, F. W.; Sinfelt, J. H. *J. Phys. Chem.* **1992**, *96*, 4960.

(24) Primet, M.; Basset, J. M.; Mathieu, M. V.; Prettre, M. *J. Catal.* **1973**, *29*, 213.

(25) Haaland, D. M.; Wiliams, F. L. *J. Catal.* **1982**, *76*, 450–465.

(26) Primet, M. *J. Catal.* **1984**, *88*, 273.

(27) Bourane, A.; Dulaurant, O.; Bianchi, D. *Langmuir* **2001**, *17*, 5496–5502.

(28) Carlsson, P.-A.; Österlund, L.; Thormählen, P.; Palmqvist, A.; Fridell, E.; Jansson, J.; Skoglundh, M. *J. Catal.* **2004**, *226*, 422.

(29) Parkyns, N. D. *J. Phys. Chem* **1971**, *75*, 526.

(30) Oh, S. H.; Mitchell, P. J.; Siewert, R. M. *J. Catal.* **1991**, *132*, 287.

(31) Becker, E.; Carlsson, P.-A.; Skoglundh, M. *Top. Catal.* **2009**, *52*, 1957.

(32) Gee, A. T.; Hayden, B. E.; Mormiche, C.; Kleyn, A. W.; Riedmuller, B. *J. Chem. Phys.* **2003**, *118*, 3334.

(33) Watson, D. T. P.; van Dijk, J.; Harris, J. J. W.; King, D. A. *Surf. Sci.* **2002**, *506*, 243.

(34) Watson, D. T. P.; Harris, J. J. W.; King, D. A. *J. Phys. Chem. B* **2002**, *106*, 3416.

(35) Walker, A.; Klötzer, B.; King, D. A. *J. Chem. Phys.* **1998**, *109*, 6879.

(36) Valden, M.; Xiang, N.; Pere, J.; Pessa, M. *Appl. Surf. Sci.* **1996**, *99*, 83 – 89.

(37) T. Kondo, T. S.; Yamamoto, S. *J. Chem. Phys.* **2003**, *118*, 760.

(38) Yoshida, H.; Yasawa, Y.; Hattori, T. *Catal. Today* **2003**, *87*, 19.

(39) Grünwaldt, J. D.; Beier, M.; Kimmerle, B.; Baiker, A.; Nachtegaal, M.; Griesebock, B.; Lützenkirchen-Hecht, D.; Stötzel, J.; Frahm, R. *Phys. Chem. Chem. Phys.* **2009**, *11*, 8779.

(40) Carlsson, P.-A.; Zhdanov, V. P.; Skoglundh, M. *Phys. Chem. Chem. Phys.* **2006**, *52*, 1962.

Figures

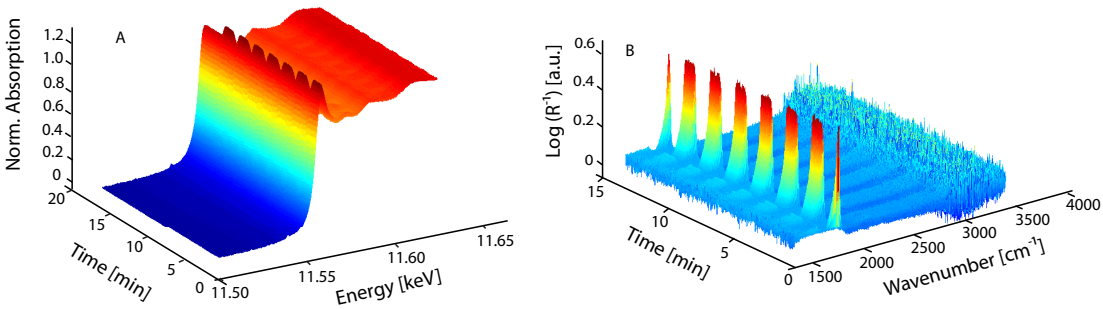

Figure 1: (A) Evolution of XANES Pt L_{III}-edge spectra and (B) IR bands in the interval 1500-4000 cm^{-1} (B) for a 4%Pt/Al_2O_3 catalyst exposed to 1000 vol.-ppm CH_4 in He while periodically switching the O_2 concentration between 0 (60 s) and 1.5% (60 s) at 280°C.

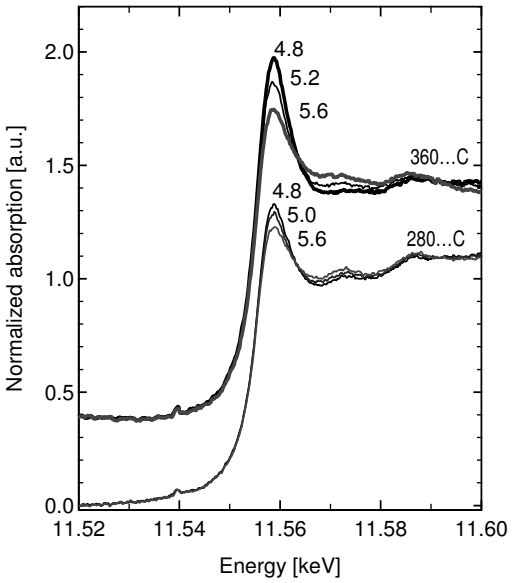

Figure 2: XANES spectra of a 4%Pt/Al_2O_3 catalyst recorded *in situ* after a switch from 1.5%O_2/0.1%CH_4 to 0.1% CH_4 at 360 and 280°C. The spectra are extracted from the oxygen pulse-response experiments shown in Figure 4 and Figure 5. The time (in min) at which each spectrum is collected is indicated.

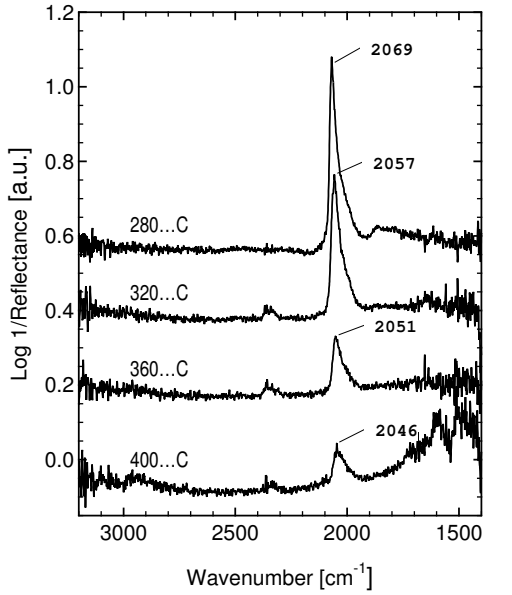

Figure 3: DRIFT spectra of a 4%Pt/Al_2O_3 catalyst recorded during 0.1% CH_4 exposure at 400, 360, 320 and 280°C. Each spectrum is extracted from the corresponding oxygen pulse-response experiments at t=5.5 min, i.e., 0.6 min after oxygen has been switched off.

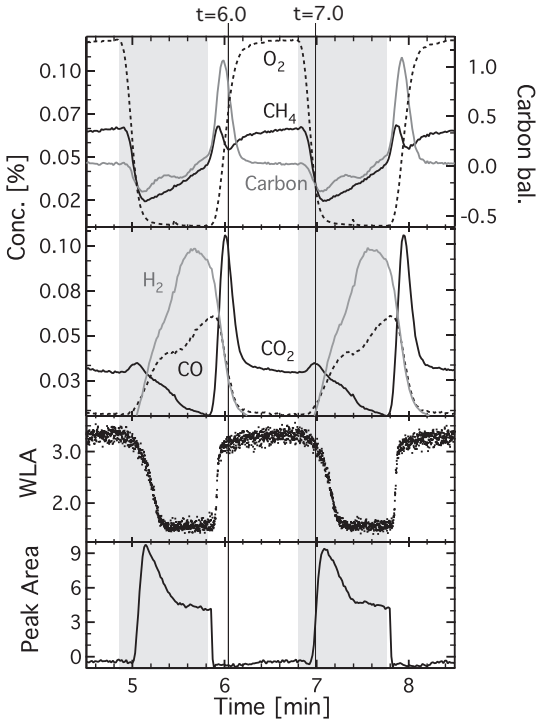

Figure 4: Oxidation of 0.1%CH_4 over a 4%Pt/Al_2O_3 catalyst at 360°C while periodically switching between 0.1% CH_4 (shaded areas) for about 1 min and 1.5%O_2/0.1%CH_4 (white areas) for about 1 min. The two upper panels show the outlet concentrations of CH_4, O_2, H_2, CO and CO_2 together with the calculated carbon balance. The two lower panels display the calculated white-line area (WLA) of the XANES Pt L_{III}-edge spectra and the integrated peak area of CO linearly adsorbed on Pt ($\tilde{\nu}_{lin}^{CO}$(Pt))

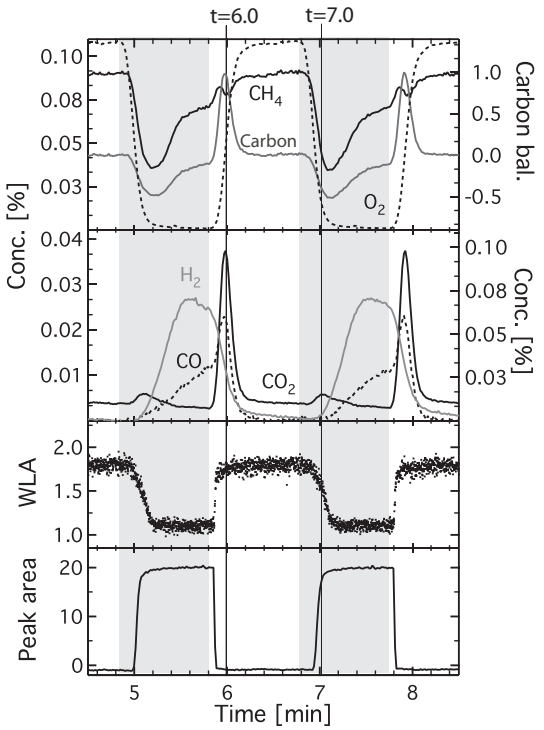

Figure 5: Oxidation of 0.1%CH_4 over a 4%Pt/Al_2O_3 catalyst at 280°C while periodically switching between 0.1% CH_4 (shaded areas) for about 1 min and 1.5%O_2/0.1%CH_4 (white areas) for about 1 min. The two upper panels show the outlet concentrations of CH_4, O_2, H_2, CO and CO_2 together with the calculated carbon balance. The two lower panels display the calculated white-line area (WLA) of the XANES Pt L_{III}-edge spectra and the integrated peak area of CO linearly adsorbed on Pt ($\tilde{\nu}_{lin}^{CO}$(Pt))

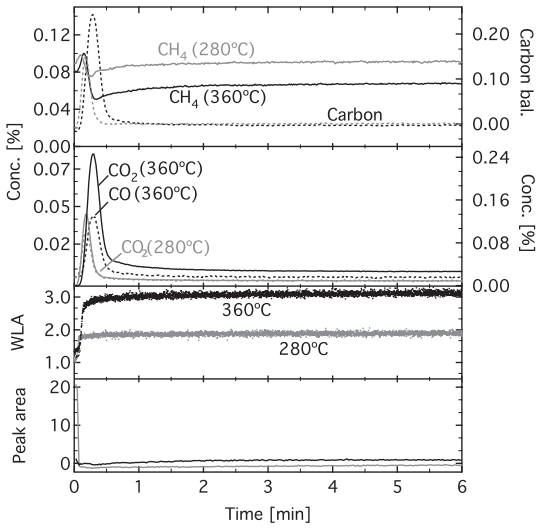

Figure 6: Oxidation of 0.1%CH_4 over a 4%Pt/Al_2O_3 catalyst at 360°C where 1.5%O_2 is introduced stepwise at t=0. The two upper panels show the outlet concentrations of CH_4, O_2, H_2, CO and CO_2, together with the calculated carbon balance. The two lower panels display the calculated white-line area of the XANES Pt L_{III}-edge spectra and the integrated peak area of CO linearly adsorbed on Pt ($\tilde{\nu}_{lin}^{CO}$(Pt)).

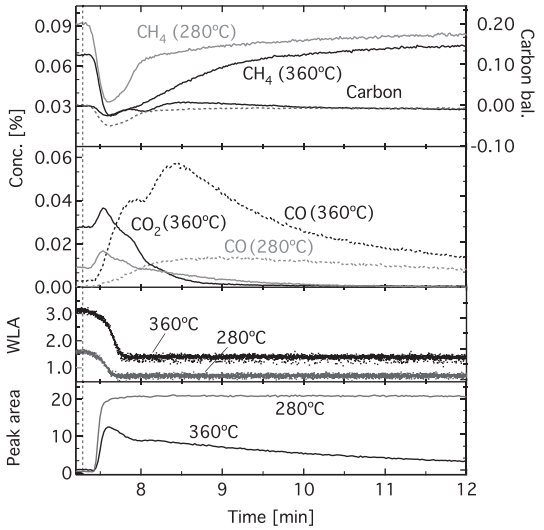

Figure 7: Oxidation of 0.1%CH_4 with 1.5%O_2 over a 4%Pt/Al_2O_3 catalyst at 280°C. Oxygen is switched off at 7.3 min. The two upper panels show the outlet concentrations of CH_4, O_2, H_2, CO and CO_2, together with the calculated carbon balance. The two lower panels display the calculated white-line area of the XANES Pt L_{III}-edge spectra and the integrated peak area of CO linearly adsorbed on Pt ($\tilde{\nu}_{lin}^{CO}$(Pt)).